Chapter 6

CHAPTER 6

Cu_2FeSnS_4 NANOPARTICLES: POTENTIAL PHOTOVOLTAIC ABSORPTION MATERIALS FOR SOLAR CELL APPLICATION

Chapter six explains the synthesis of Cu_2FeSnS_4 nanoparticles by the hydrothermal method. The analysis of the phase pure tetragonal structure by XRD and Raman spectroscopy, the UV-VIS-NIR spectral analysis and the electrochemical characterization are also deliberated in this chapter. The optimization of the Cu_2FeSnS_4 composition concentration to function as effective absorption materials for solar cell application is discussed.

6.1 INTRODUCTION

Considering the needs of the ever growing population, the demand for energy is expected to become twice in the ensuing decade. Conventional sources like fossil fuels (coal, natural fuel and gas) are being used up at a rapid pace. It is very essential to find other sources which are renewable, cheap and non-toxic. Among the various types of renewable energy, solar energy is highly attractive as it is sustainable, limitless and non-polluting. Solar cells harness the solar energy and convert it into electric energy. Initially, more than 80% of the solar industry was based on silicon solar cells. Silicon based photovoltaic cells depend on the use of thick absorber materials with an indirect band gap. However, the materials used for these absorber layers are expensive [1].

Inorganic thin-film solar cell technology depends on direct band gap absorber materials like $CuInGaSe_2$ (CIGS) [2], $Cu_2ZnSn(S,Se)_4$ (CZTS) [3, 4], Cu_2FeSnS_4 (CFTS) [5], CdTe and TiO_2, which have been widely investigated for use in thin film solar cells. Being direct optical band gap, there is no need a thick absorber film. High power conversion efficiency has been achieved with these materials. However, these solar cells cannot be used expansively as they employ relatively rare and expensive elements like indium (In) and gallium (Ga). To attain the goal of low expenditure photovoltaic technology, it is required to analyze other semiconductor materials containing sulfur, which is low- noxious, as a replacement for selenium (Se) and iron which is available in plenty in the place of

In and Ga [6]. CFTS nanoparticles are among the most promising nanomaterials for use as absorbers in thin film solar cells in view of the appropriate direct optimum band gap (Eg = 1.2 to 1.5 eV) and the profusely available and non-toxic elements [7,8, 9].

Many vacuum and non- vacuum based systems have been developed to prepared CFTS nanomaterials. Physical techniques are expensive as their operation is difficult, and complex equipment and high vacuum are needed. On the other hand, chemical techniques are simple and cheap; there is low wastage of materials and no need for vacuum, making them suitable for large scale production [10, 11]. Absorber nanomaterials show enhanced optical, chemical and mechanical properties in comparison to the bulk material. Nanomaterial technique ensures controlled nucleation and grain growth. The incorporation of dopants to control the chemical and structural properties can also been done easily. Hence, many efforts are being made to devise effective methods for the synthesis of the CFTS nanoparticles [12, 13].

Earlier researchers have used different techniques such as the solvothermal method [14], liquid reflux method [15], spray pyrolysis technique [16] and micro-wave irradiation method [17], for the preparation of the CFTS nanoparticles. In this present study, an effort has been made to prepare CFTS nanoparticles by the hydrothermal method as this technique is simple, eco-friendly, and cheap and can produce phase pure nanoparticles with high crystallinity. The precursor materials were first dissolved in the solvent and heated at the optimized time and temperature to produce the nanoparticles. The synthesized nanoparticles were dispersed in an environmentally benign solvent to produce a nanoparticle ink which was coated on ultrasonically cleaned FTO conducting glass substrates by the spin coating method [18]. Chemat KW 4A model spin- coating ensures uniformity of the thin film and produces good quality films suitable for photovoltaic applications.

6.2 MATERIALS AND METHODS

6.2.1 Preparation of Cu_2FeSnS_4 nanoparticles

The cationic precursors, copper (II) chloride ($CuCl_2.2H_2O$), iron (II) chloride ($FeCl_2.4H_2O$) and tin (II) chloride dehydrate ($SnCl_2.2H_2O$) and the anionic precursor, thiourea (CH_4N_2S), all of 99.9% purity, were procured from Sigma Aldrich chemicals.

An aqueous solution of the cationic precursors (0.02M of $CuCl_2.2H_2O$, 0.008M of $FeCl_2.4H_2O$ and 0.002M $SnCl_2.2H_2O$) was prepared by adding them in distilled water in the above sequence, allowing adequate interval to dissolve the solute. The anionic precursor thiourea (0.04 M) was next mixed in the above aqueous solution. The mixture was vigorously stirred for 3 hrs and ultrasonicated for 30 min to homogenize the solution. The obtained solution was shifted into 50 ml capacity of stainless steel autoclave and retained at 190 °C for 24 hrs. The obtained product was centrifuged and washed repeatedly using water and ethanol, and then dried at 90 °C for 7 hrs, before being used for characterization.

To convert the powder into the thin film form it was dissolved in ethanol and grinding for 3 hrs to get a homogeneous slurry, which was spin-coated on the FTO substrate at a 2000 rpm speed for 30 s. The obtained thin film was heated using a hot plate at 150 °C for 10 min to eliminate the solvent. The spin - coating and drying process for several times to obtain the required thickness. The resultant thin-film was annealed by 400 °C intended for 30 min to obtain the CFTS absorbance layer.

6.2.2 Material Characterization

Powder XRD study was carried out using the Panalytical XPERT Pro (Netherlands) X-ray diffraction system with Cu-Kα radiation source (wavelength = 1.5406 Å) operated at 45 kV. The XRD powder patterns were obtained in the scanning range of 2θ=10 - 90 ° at a scanning rate maintained at 2 °/ min. The micro- Raman spectra were obtained by using a 'WiTec alpha 300' Raman microscope (Germany) in the Raman Spectral range from 50 to 4000 cm^{-1}. The synthesized nanoparticles was studied by FE-SEM using the S4160 Hitachi equipment and the chemical composition analyzed by Bruker-4010 model EDAX analyzer. The optical UV- Vis- NIR spectra were studied using a JASCO (model V-770) UV- Vis- NIR spectrophotometer. Electrochemical measurement was done using the electrochemical workstation.

6.3 RESULT AND DISCUSSION

6.3.1 Structural analysis

The crystalline structure of the Cu_2FeSnS_4 nanoparticle and its phase were analyzed by powder XRD studies. Figure 6.1 shows the powder XRD peak positions of hydrothermally prepared nanoparticles. The CFTS powder showed strong diffraction peaks correspond to (112), (200), (201) and (312) planes. These are in good agree with the JCPDS card number: PDF 44 - 1476 in the tetragonal space group (*I-42m).* These results agree with reports in previous literature [19, 20]. The lattice parameters for the tetragonal structure were estimated using the relation,

$$\frac{1}{d^2} = \frac{h^2+k^2}{a^2} + \frac{l^2}{c^2} \tag{6.1}$$

Where, d is the interplanar spacing and h, k and *l* are the Miller indices. The lattice parameters were calculated to be a=b= 5.55 Å and c= 10.76 Å which agree with the JCPDS card values a=b= 5.43 Å and c= 10.73 Å. The crystallite size was estimate by using the Scherrer's formula,

$$D = \frac{k\lambda}{\beta cos\theta} \tag{6.2}$$

Where, D is the grain size, k is the constant (0.9), λ is the X-ray wavelength radiation and β is the FWHM of the peak. The mean crystallite sizes of the synthesized nanoparticles were calculated to be within the range from 8 to 30 nm.

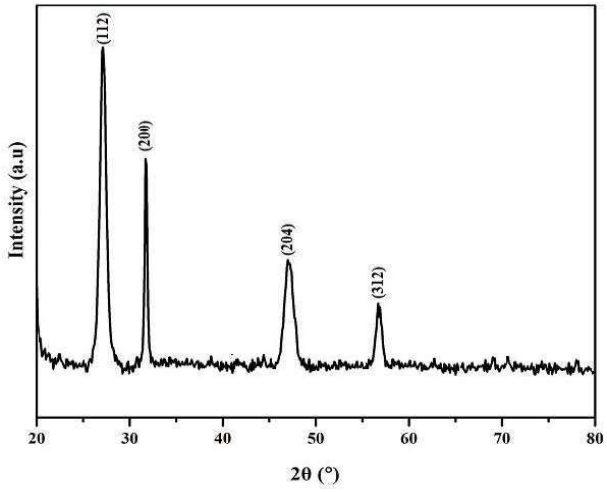

Figure 6.1 Powder XRD spectrum for CFTS nanoparticles

6.3.2 UV-VIS-NIR spectral analysis

To understand the optical absorbance properties of the synthesized CFTS powder, the UV-spectrum is recorded in the DRS mode in the wavelength ranging from 250 - 900 nm. The UV spectra obtained are shown in Figure 6.2(a). It is observed that the prepared Cu_2FeSnS_4 nanoparticles exhibit a wide absorption in the UV visible region with absorption tails that extend into longer wavelength region. The optical band gap of the CFTS nanoparticles was estimated from a plot of $(\alpha h\upsilon)^2$as a function of $h\upsilon$, where α is the absorbance, h is the Planck's constant and υ is the frequency. Here$(\alpha h\upsilon) = A(h\upsilon - Eg)^n$, where Eg (eV) is the optical band gap energy and $n = \frac{1}{2}$ for direct optical Eg semiconductor. The optical Eg was determined to be approximately 1.39 eV by extra plotting the linear part of the spectrum to zero as in Figure 6.2(b).This is close to the optimum value for high conversion efficiency [21, 22].

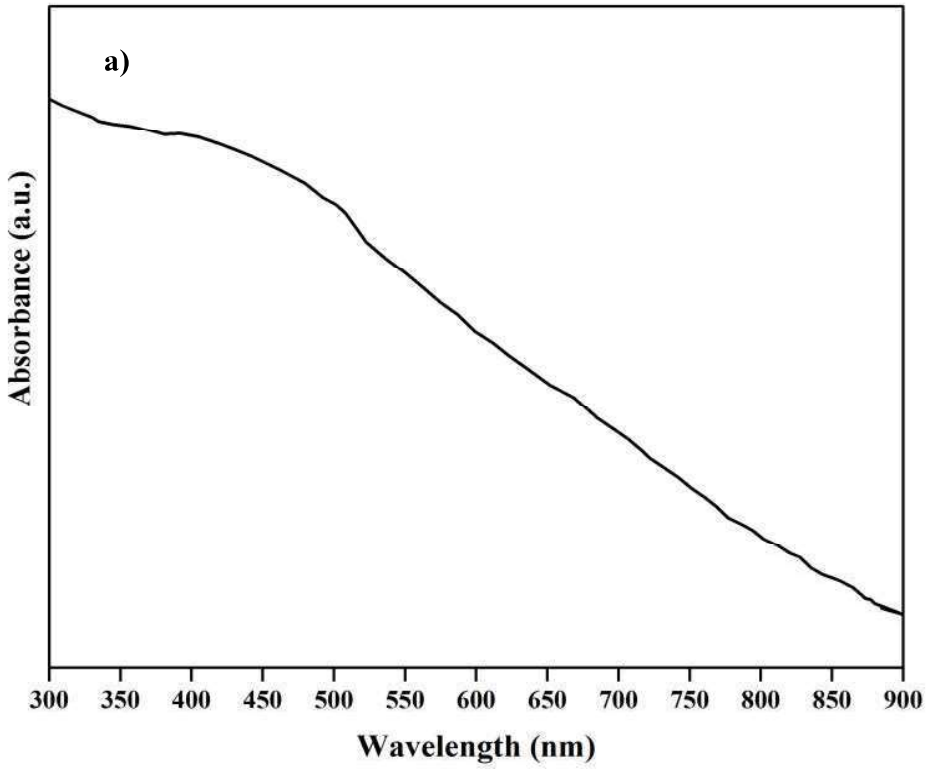

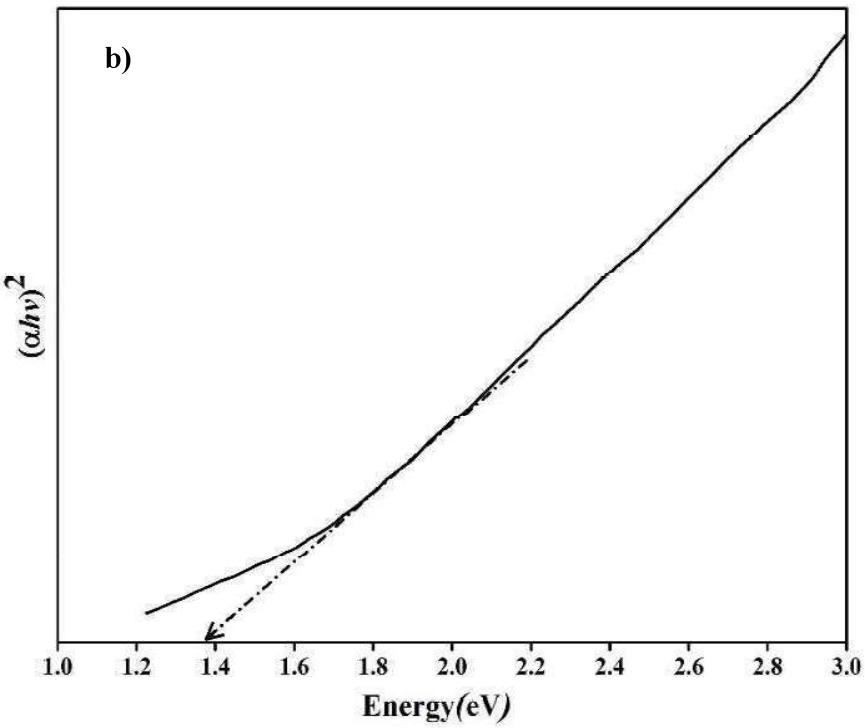

Figure 6.2 (a) Absorption spectrum and
(b) The plot of hv versus $(\alpha hv)^2$ for CFTS nanoparticles

6.3.3 Morphological and compositional analysis

The FE-SEM image of the CFTS nanoparticles is shown in Figure 6.3(a). The CFTS nanoparticles reveal slight agglomeration with irregular sphere like particle average size from 10 - 30 nm, which agrees with the XRD data. This slight agglomeration could be attributed to an increase in surface energy with decrease in size [23]. This kind of sphere like morphology enhances photon absorption and hence finds use in photovoltaic applications.

The EDAX spectrum in Figure 6.3(b) indicates peaks corresponds to copper, iron, tin and thiourea, endorsing the phase purity of the Cu_2FeSnS_4 nanoparticles. The elemental composition ratio of copper, iron, tin and thiourea in Cu_2FeSnS_4 is about 29.82: 15.93: 3.78: 50.47, which is close to the initial starting material [24].

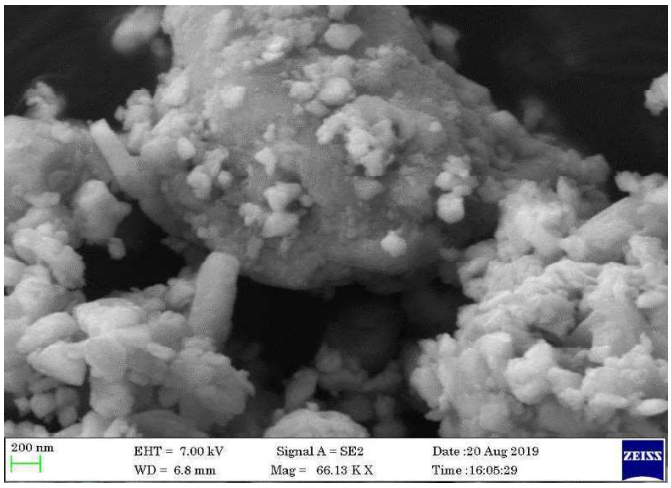

Figure 6.3(a) SEM image for CFTS nanoparticles

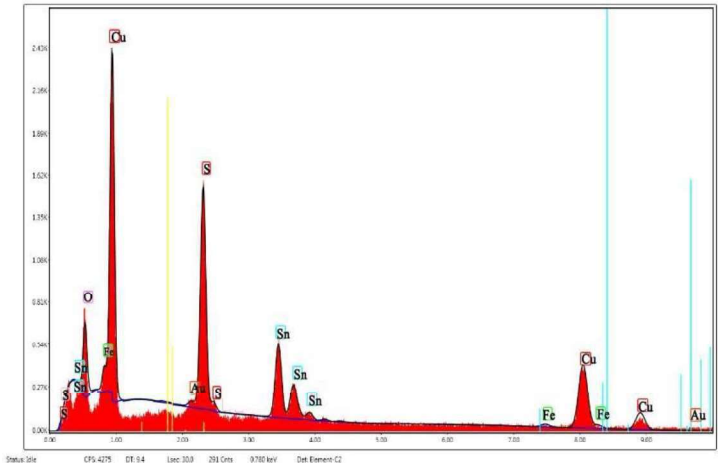

Figure 6.3(b) EDAX spectra of CFTS nanoparticles

6.3.4 Cyclic Voltammetry analysis

To study the electro catalytic ability of the Cu_2FeSnS_4 thin-film was evaluated by cyclic voltammetry measurements were performed under three electrode system with 0.1M NaOH electrolyte in the potential ranging from -1.0 V - 1.0 V with scan rates (sc) of 5 and 10 mVs^{-1}. FTO glass was used as the working electrode slurry was spin-coated onto the FTO substrate (1 cm x1 cm) while platinum wire and Ag/AgCl were employed as the counter and reference electrodes. From Figure 6.4, it is observed that for a 5 mVs^{-1} scan rate, the anodic peak is observed at 0.012 mA/cm^2 and cathodic peaks at - 0.0087 mA/cm^2 and - 0.0154 mA/cm^2. The corresponding potentialof the anodic peak is at 0.0518 V and that of the cathodic peaks are at - 0.135 V and - 0.4195 V respectively.

For a 10 mVs^{-1} scan rate, the maximum current density peaks were detected at 0.0109 mA/cm^2 (anodic peak) and - 0.0095 mA/cm^2 and - 0.0179 mA/cm^2 (cathodic peaks). The corresponding potential of the anodic peak is 0.0085 V and the cathodic peak potentials are - 0.049 V and - 0.385 V respectively (Figure 6.4). It is observed that the area under the CV curve increased with the scan rate. The cathodic peak at maximum current density indicates an electrochemical behavior and good catalytic activity of the CFTS in NaOH electrolyte.

Anima Ghosh et al [25] have reported that the cyclic voltammetric curves for copper based chalcogenide thin films show a rise in the current density when illuminated visible light. These films are used in photo-electrochemical applications. Shanlong Chen et al [26] have shown that the CV curves of CZTS CEs (counter electrode) display cathodic peaks. The analogous nature of the curves for Cu_2ZnSnS_4 and Platinum CEs indicates similar electro chemical activities.

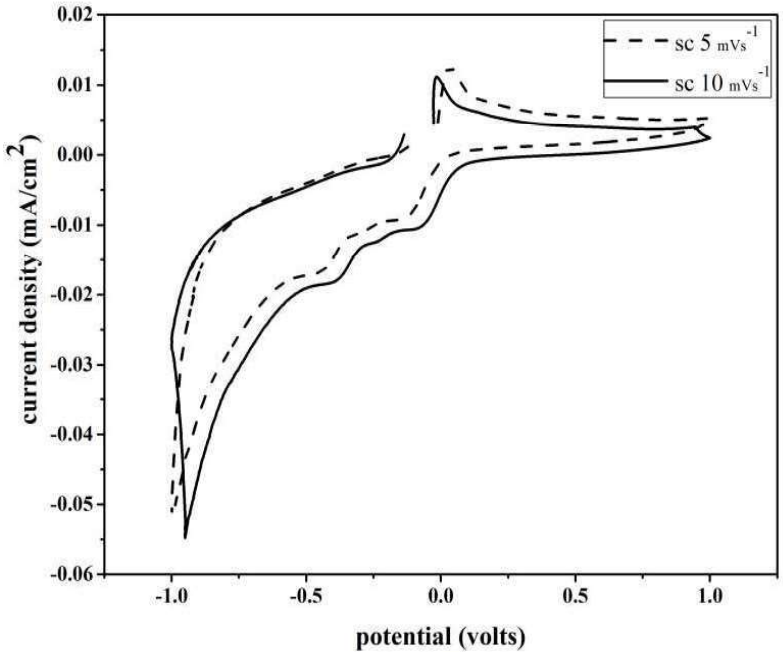

Figure 6.4 CV curves for CFTS thin film at 5 and 10 mVs^{-1}

6.4 CONCLUSION

Copper iron tin thiourea nanoparticles were prepared by a simple chemical route technique. XRD studies revealed that CFTS nanoparticles have a tetragonal structure. The synthesized CFTS nanoparticles are found to have an optical band gap of 1.39 eV which makes them potential materials for use as absorber layer in photovoltaic applications. Morphological studies show that the average size of the prepared nanoparticles is in the range from 10-30 nm. Slight agglomeration with irregular sphere like particles is observed. The cyclic voltammetry measurements show the electro-catalytic properties of the Cu_2FeSnS_4 thin-film electrode in NaOH electrolyte solution. The obtained results indicate that quaternary CFTS nanoparticles and thin film exhibit their potential for use as absorber layers in solar cell applications.

REFERENCES

1. Mitzi, D. B., Yuan, M., Liu, W., Kellock, A. J., Chey, S. J., Deline, V., & Schrott, A. G. (2008). A high-efficiency solution-deposited thin-film photovoltaic device. *Advanced Materials*, *20*(19), 3657-3662.

2. Meng, X., Deng, H., Sun, L., Yang, P., & Chu, J. (2015). Sulfurization temperature dependence of the structural transition in Cu_2FeSnS_4-based thin films. *Materials Letters*, *161*, 427-430.

3. Fernandes, P. A., Salomé, P. M. P., & Da Cunha, A. F. (2011). Study of polycrystalline Cu_2ZnSnS_4 films by Raman scattering. *Journal of alloys and compounds*, *509*(28), 7600-7606.

4. Vanalakar, S. A., Agawane, G. L., Kamble, A. S., Patil, P. S., & Kim, J. H. (2017). The green hydrothermal synthesis of nanostructured $Cu_2ZnSnSe_4$ as solar cell material and study of their structural, optical and morphological properties. *Applied Physics A*, *123*, 1-7.

5. Wang, S., Ma, R., Wang, C., Li, S., & Wang, H. (2017). Incorporation of Rb cations into Cu_2FeSnS_4 thin films improves structure and morphology. *Materials Letters*, *202*, 36-38.

6. Nilange, S. G., Patil, N. M., & Yadav, A. A. (2019). Growth and characterization of spray deposited quaternary Cu_2FeSnS_4 semiconductor thin films. *Physica B: Condensed Matter*, *560*, 103-110.

7. Agawane, G. L., Shin, S. W., Vanalakar, S. A., Moholkar, A. V., & Kim, J. H. (2014). Next generation promising $Cu_2(Zn_xFe_{1-x})SnS_4$ photovoltaic absorber material prepared by pulsed laser deposition technique. *Materials Letters*, *137*, 147-149.

8. Agawane, G. L., Vanalakar, S. A., Kamble, A. S., Moholkar, A. V., & Kim, J. H. (2018). Fabrication of $Cu_2(Zn_xMg_{1-x})SnS_4$ thin films by pulsed laser deposition technique for solar cell applications. *Materials Science in Semiconductor Processing*, *76*, 50-54.

9. Vanalakar, S. A., Patil, P. S., & Kim, J. H. (2018). Recent advances in synthesis of Cu_2FeSnS_4 materials for solar cell applications: a review. *Solar Energy Materials and Solar Cells*, *182*, 204-219.

10. Miao, X., Chen, R., & Cheng, W. (2017). Synthesis and characterization of Cu_2FeSnS_4 thin films prepared by electrochemical deposition. *Materials Letters*, *193*, 183-186.

11. Chatterjee, S., & Pal, A. J. (2017). A solution approach to p-type Cu_2FeSnS_4 thin-films and pn-junction solar cells: role of electron selective materials on their performance. *Solar Energy Materials and Solar Cells*, *160*, 233-240.

12. Lydia, R., & Sreedhara Reddy, P. (2013). Effect of pH on the characteristics of Cu_2ZnSnS_4 nanoparticles. *International Scholarly Research Notices*, *2013*.

13. Belaqziz, M., Medjnoun, K., Djessas, K., Chehouani, H., & Grillo, S. E. (2018). Structural and optical characterizations of Cu_2SnS_3 (CTS) nanoparticles synthesized by one-step green hydrothermal route. *Materials Research Bulletin*, *99*, 182-188.

14. Nazari, P., Yazdani, A., Shadrokh, Z., Nejand, B. A., Farahani, N., & Seifi, R. (2017). Band gap engineering of $Cu_3Fe_xSn_{(1-x)}S_4$: A potential absorber material for solar energy. *Journal of Physics and Chemistry of Solids*, *111*, 110-114.

15. Zhou, J., Ye, Z., Wang, Y., Yi, Q., & Wen, J. (2015). Solar cell material Cu_2FeSnS_4 nanoparticles synthesized via a facile liquid reflux method. *Materials letters*, *140*, 119-122.

16. El Fidha, G., Bitri, N., Mahjoubi, S., Abaab, M., & Ly, I. (2018). Effect of the spraying temperatures and the sulfurization on the properties of the absorber Cu_2FeSnS_4 thin films in a solar cell. *Materials Letters*, *215*, 62-64.

17. Guan, H., Shi, Y., Jiao, B., Wang, X., & Yu, F. (2014). Flower-like Cu_2FeSnS_4 particles synthesized by microwave irradiation method. *Chalcogenide Lett*, *11*(1), 9-12.

18. Liu, W., Guo, B., Mak, C., Li, A., Wu, X., & Zhang, F. (2013). Facile synthesis of ultrafine Cu_2ZnSnS_4 nanocrystals by hydrothermal method for use in solar cells. *Thin Solid Films*, *535*, 39-43.

19. Adelifard, M. (2016). Preparation and characterization of Cu_2FeSnS_4 quaternary semiconductor thin films via the spray pyrolysis technique for photovoltaic applications. *Journal of analytical and applied pyrolysis*, *122*, 209-215.

20. Jiang, X., Xu, W., Tan, R., Song, W., & Chen, J. (2013). Solvothermal synthesis of highly crystallized quaternary chalcogenide Cu_2FeSnS_4 particles. *Materials Letters*, *102*, 39-42.

21. Cao, M., Li, C., Zhang, B., Huang, J., Wang, L., & Shen, Y. (2015). PVP assisted solvothermal synthesis of uniform Cu_2FeSnS_4 nanospheres. *Journal of Alloys and Compounds*, *622*, 695-702.

22. Zhou, J., Yu, S., Guo, X., Wu, L., & Li, H. (2019). Preparation and characterization of Cu_2FeSnS_4 thin films for solar cells via a co-electrodeposition method. *Current Applied Physics*, *19*(2), 67-71.

23. Phaltane, S. A., Vanalakar, S. A., Bhat, T. S., Patil, P. S., Sartale, S. D., & Kadam, L. D. (2017). Photocatalytic degradation of methylene blue by hydrothermally synthesized CZTS nanoparticles. *Journal of Materials Science: Materials in Electronics*, *28*, 8186-8191.

24. Wang, W., Shen, H., Yao, H., & Li, J. (2014). Preparation and properties of Cu_2FeSnS_4 nanocrystals by ultrasound-assisted microwave irradiation. *Materials Letters*, *125*, 183-186.

25. Ghosh, A., Chaudhary, D. K., Biswas, A., Thangavel, R., & Udayabhanu, G. (2016). Solution-processed Cu_2XSnS_4 (X= Fe, Co, Ni) photo-electrochemical and thin film solar cells on vertically grown ZnO nanorod arrays. *RSC Advances*, *6*(116), 115204-115212.

26. Chen, S., Xu, A., Tao, J., Tao, H., Shen, Y., Zhu, L., ... & Pan, L. (2015). In-situ and green method to prepare Pt-free Cu_2ZnSnS_4 (CZTS) counter electrodes for efficient and low cost dye-sensitized solar cells. *ACS Sustainable Chemistry & Engineering*, *3*(11), 2652-2659.